IEEE Transactions on Industrial Electronics, Vol. 64, Iss. 10, October 2017, pp.7984-7993
DOI:10.1109/TIE.2017.2694414

High-Precision Hydraulic Pressure Control Based on Linear Pressure-Drop Modulation in Valve Critical Equilibrium State

Chen Lv, *Member, IEEE*, Hong Wang and Dongpu Cao, *Member, IEEE*

***Abstract*—High precision and fast response are of great significance for hydraulic pressure control in automotive braking systems. In this paper, a novel sliding mode control based high-precision hydraulic pressure feedback modulation is proposed. Dynamical models of the hydraulic brake system including valve dynamics are established. An open loop load pressure control based on the linear relationship between the pressure-drop and coil current in valve critical open equilibrium state is proposed, and also experimentally validated on a hardware-in-the-loop test rig. The control characteristics under different input pressures and varied coil currents are investigated. Moreover, the sensitivity of the proposed modulation on valve's key structure parameters and environmental temperatures are explored with some unexpected drawbacks. In order to achieve better robustness and precision, a sliding mode control based closed loop scheme is developed for the linear pressure-drop modulation. Comparative tests between this method and the existing methods are carried out. The results validate the effectiveness and superior performance of the proposed closed loop modulation method.**

***Index Terms*— Sliding mode control, linear pressure-drop modulation, switching valve, hardware-in-the-loop test, experimental validation.**

I. Introduction

High precision and fast response are crucial performances for actuators in most hydraulic control system domains, including automotive braking systems [1]-[4]. Due to the significant properties such as high power density, flexibility, high stiffness, and low cost, hydraulic systems, have been widely used in vehicle braking control [5], [6]. The demand for brake safety, ride comfort, and energy regeneration calls more high performance and highly efficient actuators for control systems [7]-[9]. Thus, the system design and precision control of brake devices have been drawn great attention during the past few years [10]-[12].

To achieve high-performance modulation of brake pressure, proportional valve with digital control is the most effective and direct way [13]. It can achieve a continuous control of hydraulic fluid flow, leading to a linear control of hydraulic pressure. Although some of the proportional valves have been developed with application of advanced nonlinear control techniques, this kind of approach is usually highly cost and complicated for hardware [14]. These restrict their practical applications and instead make switching valves driven by pulse width modulated (PWM) inputs widely used [15]. By utilizing switching valves with PWM control, the cost and complexity of the system can be effectively reduced. However, because the PWM duty cycle is regulated, pressure modulation is not a continuous process with only the mean value of the valve opening being controlled. Therefore, the load pressure obtained under PWM control is non-linear and imprecise.

To improve the hydraulic pressure control performance, researchers worldwide have been carried out comprehensive research in design and control method of hydraulic actuators. In [16], a position and a velocity observer combined in a cascade structure were developed for valves, and applied in a sensorless engine control system. A valve spool position observer was developed in [17]. Combined with the sliding mode control techniques, it was validated to improve pressure modulation accuracy. In [18], a pressure difference limiting control method was proposed for on/off solenoid valves to improve the brake blending control performance. However, the hydraulic pressure was open loop controlled, which was not robust enough under external disturbances. In [19], a modified PWM algorithm was proposed in order to increase response of on/off valves. And to improve the system robustness under various external loads, a switching algorithm using a learning vector quantization neural network was also developed. In [20], a novel fuzzy-logic based control method for controlling the transport platform of a pneumatic cushion system was presented. Experimental results show that the control performance and system stability were effectively improved. In [21], a novel energy-saving control strategy with a novel hardware configuration consisting of five

Manuscript received August 09, 2016; revised March 15, 2017; accepted March 29, 2017.

Chen Lv, and Dongpu Cao are with Advanced Vehicle Engineering Centre, Cranfield University, Bedfordshire MK43 0AL, United Kingdom (e-mail:c.lyu@cranfield.ac.uk, d.cao@cranfield.ac.uk). (*Corresponding author is Dongpu Cao.)

Hong Wang is with Mechanical and Mechatronics Engineering with the University of Waterloo, 200 University Avenue West Waterloo, ON, N2L 3G1, Canada (e-mail: hong.wang@uwaterloo.ca).

cartridge valves and one accumulator was proposed for the accurate tracking in a hydraulic system. Nevertheless, the existing research on switching valve control is mainly focused on PWM based novel method and algorithm design; the linear modulation can be hardly achieved.

To further enhance the pressure control precision of on/off valves, a novel closed loop modulation method indirectly through the linear control of differential pressure is proposed and experimentally studied in this article. A nonlinear system model with valve dynamics, which reveals the electrical, mechanical, and hydraulic coupled mechanisms, has been developed. On this basis, a linear relationship between the pressure-drop and coil current in valve critical equilibrium state is proposed and validated on a hardware-in-the-loop (HiL) test rig. Moreover, the characteristics of the proposed control with varied operation conditions are investigated. Some potential drawbacks and issues are also discussed. In order to achieve better robustness and control precision, a closed loop modulation scheme based on the linear regulation of the differential pressure is developed with a sliding mode controller designed. Some of the test results and analyses are also presented in this article.

The outline of the work is organized as follows: In Section II, the system's dynamical model including the electrical, mechanical, and hydraulic coupled subsystems is established; In Section III, an open loop load pressure control based on the linear relationship between the pressure drop and coil current is proposed and experimentally validated; In Section IV, the characteristics of the open loop load pressure control are investigated; In Section V, a sliding mode control based closed loop modulation scheme is developed for enhancing the robustness and precision of the linear pressure drop regulation.

II. System Description and Modelling

In order to explore and analyze the characteristics of linearity between the pressure drop and coil current, appropriate dynamic models of the hydraulic system including valve actuators need to be built up.

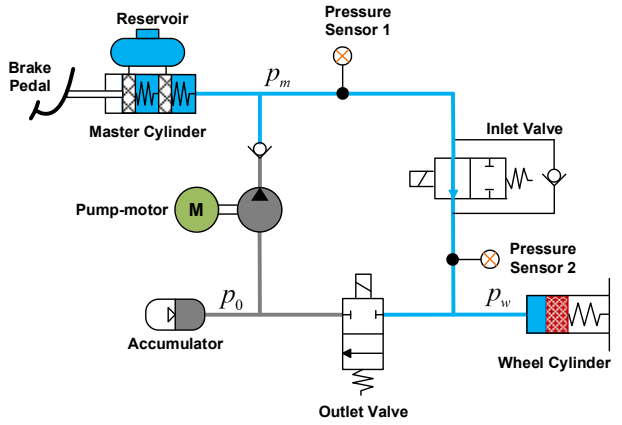

Fig. 1. Schematic diagram of the hydraulic braking control system.

The ABS hydraulic modulator is a typical hydraulic control system of automobile. Take the inlet valve of an ABS modulator as a case to study, and the schematic diagram of the hydraulic system selected is shown in Fig. 1. The inlet valve is set in between master cylinder and wheel cylinder. p_m is the master cylinder pressure, which is regarded as the input pressure of the inlet valve, can be detected by the pressure sensor 1. p_w is the wheel cylinder pressure, which is the load pressure in the case-study hydraulic control system and can be detected by the pressure sensor 2. When driver depresses the brake pedal, the pressure p_m is built up in the master cylinder and applied in the downstream circuit. The opening area of the inlet valve is controlled based on the braking control strategy, modulating the load pressure p_w in the wheel cylinder to track the expected value.

A. Valve dynamics modelling

Take the inlet valve of the hydraulic braking system, a typical normally opened outflow valve shown in Fig. 1, as an example. As shown in Fig. 2, the OX coordinate system of the valve axial movement is established with regard to the endpoint of the spherical surface in valve closed state as the coordinate origin. OX is defined as the positive direction for valve opening, pointing upwards.

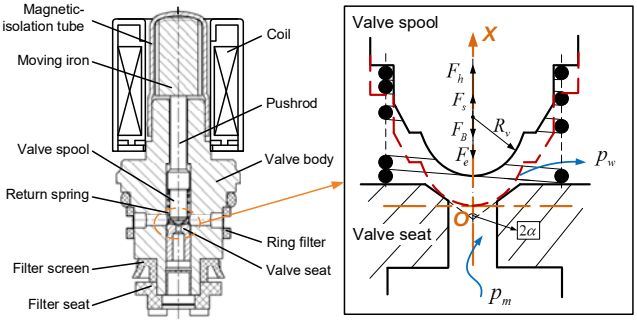

Fig. 2. Diagram of the inlet valve with the OX coordinate system of the valve axial movement.

During valve movement, considering the forces exerted on the spool, the valve dynamics in axial direction can be given by:

$$m_v \cdot \frac{d^2 x_v}{d^2 t} = -F_e + F_s + F_h - F_B \tag{1}$$

where, m_v is the total mass of valve spool, x_v is the axial displacement, F_e is the electromagnetic force, F_s is the spring force, F_h is the axial hydraulic force, and F_B is the viscous force.

The electromagnetic force acting on valve spool is mainly related to the coil current i, turn number N, the air gap length l, and the magnetic reluctance of air gap R_g. The amount of electromagnetic force can be given by [22], [23]:

$$F_e = (iN)^2 / (2R_g l) \tag{2}$$

In order to reduce the complexity of modelling, the above nonlinear representation of the electromagnetic force can be simplified using the following approximation [18]:

$$F_e = K_i i(t) + K_{xe} x_v(t) \tag{3}$$

where, K_i is the current-force coefficient, and K_{xe} is the displacement-force coefficient. The values of these two parameters can be obtained through experimental calibration.

Since the inlet valve is normally opened, in the coordinate system established, the resistant force generated by the spring and applied in the spool can be calculated by:

$$F_s = K_s(x_0 + x_m - x_v) \tag{4}$$

where, x_0 is the spring preload displacement, x_m and x_v are the maximum and the actual displacements of the return spring, respectively, and K_s is the stiffness coefficient.

There is another resistance, i.e. the viscous force. It is applied on the spool only when the valve is open and the flow commences. Its amount is decided by the fluid viscosity and the axial movement velocity of valve speed, as shown in equation (5).

$$F_B = B\frac{dx_v}{dt} \tag{5}$$

where, B is the viscous damping coefficient.

The axial hydraulic force, generated by the hydraulic fluid and exerted on the spool, can be divided into two parts: the static part $F_{h,st}$ and the transient part $F_{h,trans}$ [24], as shown in equation (6).

$$F_h = F_{h,st} + F_{h,trans} \tag{6}$$

The axial static hydraulic force is caused by the time-invariant fluid flowing through the orifice. According to momentum theory, it can be calculated by [25]:

$$F_{h,st} = \pi R_v^2(\cos\alpha)^2\Delta p - \rho q_v(v_j\cos\alpha - v_0) \tag{7-1}$$

$$v_j = \frac{q_v}{A_j},\ v_0 = \frac{q_v}{A_0} \tag{7-2}$$

$$A_j = \frac{\pi d_m}{R_v}\sqrt{R_v^2 - \frac{d_m^2}{4}}x_v \tag{7-3}$$

where, ρ is the density of the hydraulic fluid, α is the cone angle of valve seat, R_v is the sphere radius of valve spool, q_v is the flow across the valve, v_0 is the average flow velocity at the inlet section of the valve, A_0 is the inlet section area, v_j is the average flow velocity at the throttle section, A_j is the area of the throttle section, and d_m is the average diameter of the valve seat.

For the transient hydraulic force, it is resulted by the time-varying flow. Its amount is related to the valve opening, and can be given by [26]:

$$F_{h,trans} = -\rho L\frac{dq_v}{dt} \tag{8}$$

where, L is the damping length, which a geometric dimension representing the axial length between the inlet and outlet flows.

The value of the flow depends on the differential pressure across the valve orifice, which can be given by [27]:

$$q_v = C_d A_j\sqrt{\frac{2\Delta p}{\rho}} \tag{9}$$

where, C_d is the discharge coefficient.

Then by combining equations (7), (8), and (9), the overall axial hydraulic force can be obtained as:

$$F_h = \pi R_v^2(\cos\alpha)^2\Delta p - 2C_d^2 A_j\Delta p\cos\alpha(1-\frac{A_j}{A_0}) - \rho L\frac{dq_v}{dt} \tag{10}$$

B.Load pressure modelling

In this study, the load pressure of the whole hydraulic braking system is the wheel pressure, which is also the outlet pressure of inlet valve, as shown in the schematic diagram of Fig. 1. The load pressure is mainly decided by the amount of the fluid flow. The relationship between the load pressure and the flow can be given by the following equations:

$$\Delta p = p_m - p_w \tag{11}$$

$$A_w dx = q_v dt \tag{12}$$

$$dp_w = \frac{k_w}{A_w}dx \tag{13}$$

where, k_w is the spring stiffness of the wheel cylinder, A_w is the cross-sectional area of wheel cylinder.

Combining equations (9), (12), and (13), the load pressure dynamics can be obtained as:

$$\frac{dp_w}{dt} = \frac{k_w}{A_w^2}C_d A_j\sqrt{\frac{2\Delta p}{\rho}} \tag{14}$$

Some key parameters of the inlet valve are listed in Table 1.

TABLE 1
KEY PARAMETERS OF THE INLET VALVE

Parameter	Value
Big-endian diameter of valve seat (d_2/mm)	1.2
Coil resistance (R/Ω)	7.4
Cone angle of valve seat (α/degree)	114
Current-force coefficient (K_i/N/A)	13.5
Displacement-force coefficient (K_{xe}/N/mm)	0.012
Inlet section area (A_0/mm^2)	0.38
Little-endian diameter of valve seat (d_1/mm)	0.65
Mass of valve spool (m/g)	2.1
Max displacement of spool (x_m/mm)	0.3
Pretension displacement of spring (x_0/mm)	3.1
Sphere diameter (d_v/mm)	1.588
Spring stiffness (K_s/N/mm)	0.34
Turn number (N)	450

III. LINEAR PRESSURE-DIFFERENTIAL CONTROL IN VALVE CRITICAL OPEN EQUILIBRIUM STATE

Based on the dynamical system models established above, an open loop control law for load pressure based on the linear pressure-drop modulation in valve critical open equilibrium state is explored and experimentally validated in this section.

A.Critical open equilibrium state of valve

In valve's fully closed state, the opening area of the orifice is zero without fluid flow, and the spool is settled on the valve seat, as Fig. 3 shows.

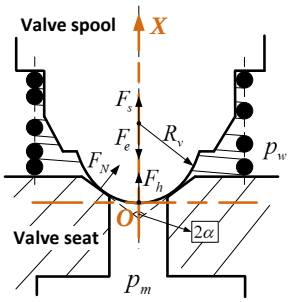

Fig. 3. The fully closed state of the inlet valve with the developed coordinate system.

Thus, the viscous force, which is only generated during valve movement, doesn't exist, but the supportive force by valve seat appears. Then, the axial balance equation of valve spool can be expressed as:

$$-F_e + F_s + F_h + F_N\sin\alpha = 0 \tag{15}$$

where, F_N is the supportive force.

Deriving from valve's closed state, there exists a critical open equilibrium state. It is actually a transient state between valve

fully closed and fully opened. When valve reaches this critical open equilibrium state, although the orifice is still closed, it is just about to open. The valve opening is remained at zero, and there exists no fluid flow in the current condition, but the supportive force disappears. And the axial balance equation of the spool can then be written as:

$$-F_e + F_s + F_h = 0 \tag{16}$$

B. Linear Pressure-Drop Control

Under the above defined critical open equilibrium state, in the coordinate system built, the valve spool velocity and displacement are zero, and the spring is stretched to spool's maximum displacement. Then, based on equations (3), (4), and (10), the electromagnetic force, the spring force, and the hydraulic force in this state can be calculated as follows, respectively.

$$F_e = K_i i(t)|_{x_v=0} \tag{17}$$

$$F_s = K_s(x_0 + x_m)|_{x_v=0} \tag{18}$$

$$F_h = \pi R_v^2 (\cos\alpha)^2 \Delta p|_{A_j=0, q_v=0} \tag{19}$$

Combing (17)-(19), then axial balance equation of the spool in valve critical open equilibrium state shown in equation (16) can be re-written as:

$$-K_i i + K_s(x_0 + x_m) + \pi R_v^2 (\cos\alpha)^2 \Delta p = 0 \tag{20}$$

Reforming the equation above equation, a linear relationship between the differential pressure and the coil current in valve critical open equilibrium state can be obtained, as equation (21) shows.

$$i = \frac{\pi R_v^2 (\cos\alpha)^2}{K_i}\Delta p + \frac{K_s}{K_i}(x_0 + x_m) \tag{21}$$

Moreover, if the input pressure can be detected, by regulating the coil current, then a linear modulation of the load pressure has a great potential be indirectly obtained through the above linear pressure drop control, as equation (22) shows.

$$\begin{aligned} p_{out} &= p_{in} - \Delta p \\ &= p_{in} - \frac{K_i i}{\pi R_v^2 (\cos\alpha)^2} + \frac{K_s(x_0 + x_m)}{\pi R_v^2 (\cos\alpha)^2} \end{aligned} \tag{22}$$

C.Experimental validation

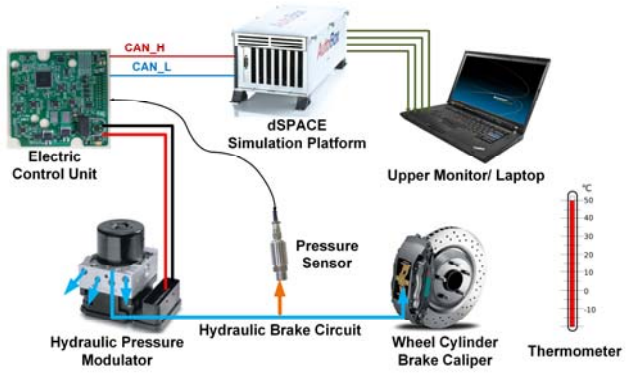

Fig. 4. Schematic diagram of the hardware-in-the-loop testing system.

To validate the above theoretical analysis of the linear differential pressure modulation, as well as the dynamic system models built, a HiL test rig is established and experimental tests are carried out. As shown in Fig. 4, the HiL experimental system is comprised of an upper computer, a lower computer, an electric control unit, real hydraulic braking control actuators, pressure sensors and a thermometer.

The upper computer is utilized to monitor the testing process and save experimental data. The lower computer adopted in this study is an AutoBox simulation platform from dSPACE. Virtual models with high-level tasks and environments are contained in AutoBox, simulating different driving scenarios, including different deceleration demands, road adhesion coefficient, and initial deceleration speed. The electric control unit consists of a microcontroller, its peripheral circuits and some processing-driving circuits, directly driving the actuators in the hydraulic pressure modulator. Two hydraulic pressure sensors, namely pressure sensor 1 and pressure sensor 2 as depicted in Fig. 1, are utilized to measure the master cylinder pressure and the wheel cylinder pressure, respectively. The pressure range of the sensor is 0-10 MPa, and the accuracy is 0.1%. A thermometer is used for measuring the environmental temperature during testing. The electric control unit communicates with the AutoBox via CAN bus, and the sampling rate of the test rig is 100 Hz. Finally, the HiL experimental platform is established, as shown in Fig. 5.

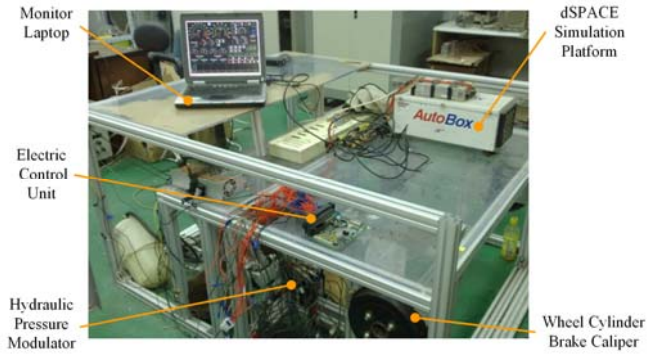

Fig. 5. Photograph of the developed hardware-in-the-loop test rig.

Based on the established test platform, the effectiveness of the valve dynamic model is validated at first. As shown in Fig. 6, the inlet valve of the hydraulic pressure modulator and the valve dynamic model built in MATLAB/Simulink are fed with the same control input of varied coil current. And the simulation results of the inlet pressure, load pressure and pressure drop match with the real experimental data very well during the dynamic modulation process, demonstrating the feasibility and correctness of the model.

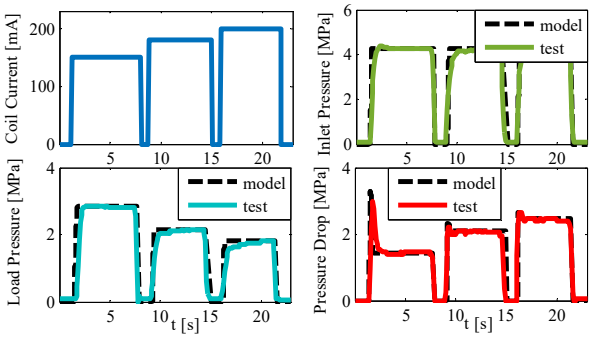

Fig. 6. Experimental and simulation results of the hydraulic system under dynamic input of coil current.

Furthermore, according to equation (21) in the above theoretical analysis, the experimental tests are carried out with

the inlet valve being controlled under its critical open equilibrium state. According to the results shown in Fig. 7, the experimental results of the linear correspondence between the coil current and the differential pressure of the switching valve match the simulation data quite well, validating the correctness of the linear pressure drop control mechanism proposed.

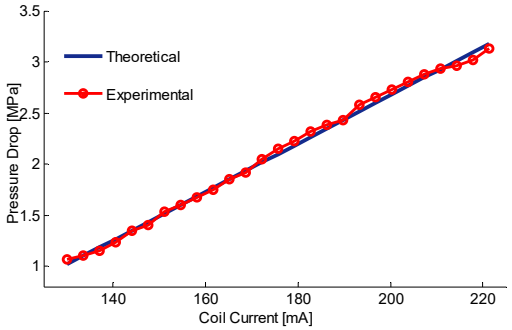

Fig. 7. Experimental and theoretical results of the linear differential pressure modulation in valve's critical open equilibrium state.

IV. Performance Analysis of the Linear Pressure-Drop Modulation

For the overall hydraulic control system studied, there are two variables that can be controlled, namely, the inlet pressure (master cylinder pressure) and coil current. Thus, based on the simulation models built and verified above, characteristics and control performance of the linear modulation of the pressure drop in valve's critical open equilibrium state are analyzed as follows.

A.Control performance under different coil currents

The control performance of the pressure drop under different coil current inputs is investigated. In the experiments, the supplied pressure at the inlet port is set as a ramp input stabilizing at 3 MPa. Different values of the coil current are tested (150 mA, 180 mA and 210 mA), and the results are shown in Fig. 8.

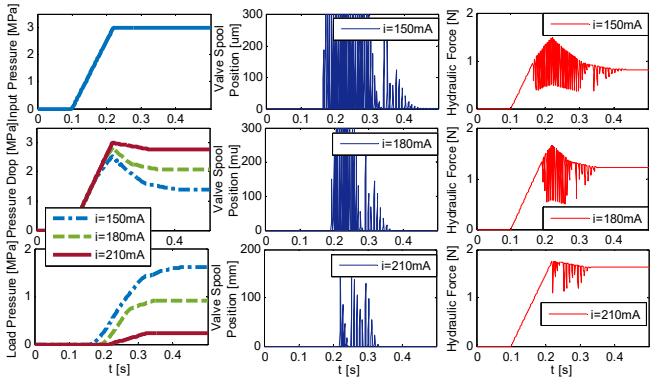

Fig. 8. Results of the control performance under different coil currents.

With an increase in the coil current from 150 mA to 210 mA, the corresponding pressure drop across the valve then increases from 1.39 MPa to 2.77 MPa, resulting in the steady state load pressure changing from 1.61 MPa to 0.23 MPa. In the condition with coil current of 210 mA, the smaller spool position indicates a decreased orifice passage area. Furthermore, according to Fig. 8, as the coil current rises, the amplitude of the hydraulic force exerting on the spool increases with the modulation duration becoming shorter.

B.Control performance under different input pressures

The responses of the corresponding pressure drop across the valve under different inlet pressures are investigated. In the test, the coil current is controlled at a fixed value of 150 mA, and the input pressures are taken as ramp inputs which finally stabilizes at 1 MPa, 2 MPa and 3 MPa, respectively. The results are illustrated in Fig. 9.

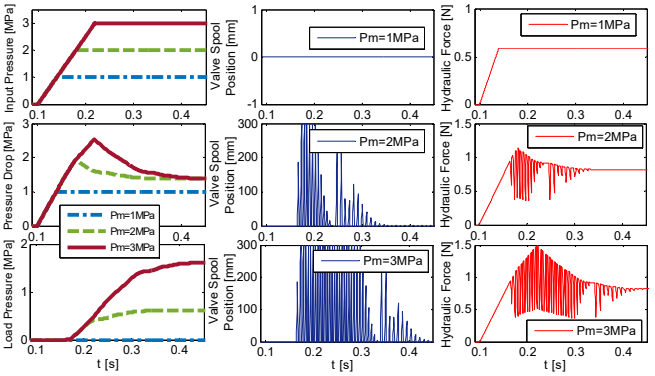

Fig. 9. Results of the control performance under different input pressures.

According to the results, under the situation with input pressure of 1MPa, the load pressure keeps at 0. This is because the controlled 150 mA coil current corresponds to a pressure drop of 1.4 MPa, which is larger than the input pressure. Thus, valve remains closed during the whole process, resulting in a zero load pressure. While in the conditions with varied input pressures at 2 MPa and 3 MPa, each corresponding pressure drop finally levels off at the same value of 1.2 MPa, indicating that the final differential pressure is only related to the coil current. However, it does take longer time for the load pressure to reach the steady state under a higher inlet pressure.

C.Control performance under different input pressures and different coil currents

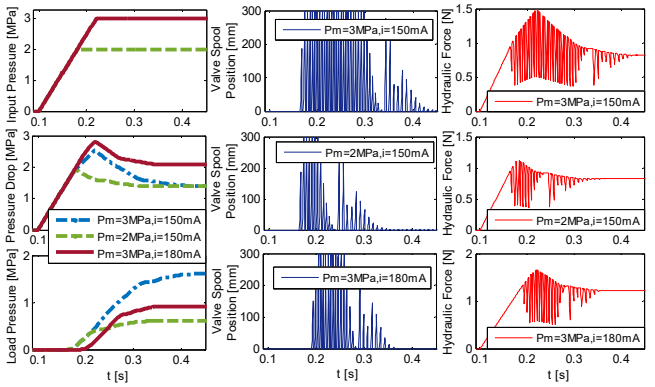

Fig. 10. Results of the control performance under different input pressures and different coil currents.

The responses of the pressure drop across the valve under different coil currents and different inlet pressures are also studied. Three test scenarios, namely the input hydraulic pressure of 3 MPa with the coil current at 150mA, the input

pressure of 2 MPa with the coil current at 150mA, and the input pressure of 3 MPa with the coil current at 180mA, are carried out, respectively. The results illustrated in Fig. 10 further demonstrate that the final differential pressure is only related to the coil current.

D.Parametric sensitivity analysis

The control performance and the parametric sensitivity of the proposed linear modulation are further explored, which can be used for validating the control strategy among various parameters of valves. The effects of some key structure parameters, including the cone angle of the valve seat, the spring stiffness, and the sphere diameter of the valve spool are studied as follows.

1) Cone angle of the valve seat

With the value selection of the cone angle of the valve seat at 112°, 114° and 116°, the experiments are carried out. As shown in Fig. 11 (a), the variation in the cone angle of the valve seat has slight impacts both on the corresponding differential pressure and the system's response during modulation. As the cone angle increases, the corresponding pressure drop in valve critical equilibrium state becomes larger with a relatively faster system response. This is because that a bigger cone angle results in a larger flow across the valve.

2) Spring stiffness coefficient

Experiments are also carried out in the situations with different selections of the spring stiffness coefficient at 330N/m, 340N/m and 350N/m, respectively. Based on the exploration results shown in Fig. 11 (b), although the effects are quite small, a larger spring stiffness coefficient do reduces the differential pressure by affecting valve dynamics in the axial direction. As the spring stiffness increases, the growing spring force counteracts a larger part of electromagnetic force, leading to a reduction in the pressure drop limiting ability.

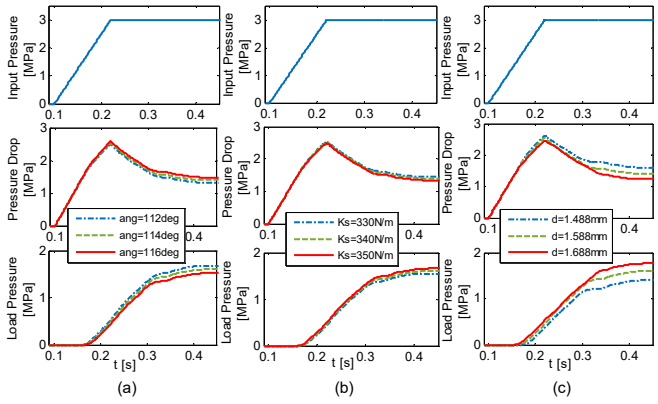

Fig. 11. Results of parametric sensitivity of the linear differential pressure modulation.

3) Spool diameter

With different selections of the spool diameter at 1.488mm, 1.588mm and 1.688mm, the experiments are carried out. The exploration results shown in Fig. 11 (c) indicates that the corresponding pressure drop is very sensitive to the variation of the spool diameter. Compared to the other two situations, in the one with a larger spool diameter at 1.688mm, the corresponding pressure drop significantly decreases, resulting in the load pressure converging to a much higher value. The reason for this phenomenon is because in valve critical open equilibrium state, a larger spool diameter generates a greater hydraulic force acting on valve, weakening the differential pressure limiting effect.

E.Temperature sensitivity experiment

Since the temperature condition significantly affects the control performance and functionality of the electro-mechanical system, the impacts of distinguished temperatures on the characteristics of the linearity between coil current and pressure drop are also investigated. HiL tests are carried out throughout the whole year with environmental temperatures varying. Four different temperature conditions, namely -3℃, +3℃, +13℃, and +24℃, are sampled. Fig. 12 shows the experimental results.

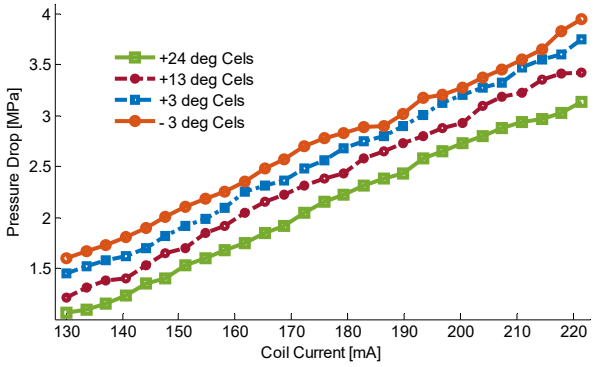

Fig. 12. Experimental results of the pressure drop linearity under varied environmental temperatures.

Based on the experimental exploration, the curve of the linear correspondence moves up significantly as the temperature decreases. However, the linear relationship between coil current and pressure drop is still kept well at different temperatures. The main reason for this phenomena is because the resistance of the coil increases when temperature climbs up [28], which results in a smaller electro-magnetic force, weakening the capability to limit the pressure drop across the valve.

Remark 1: According to the above testing and analysis in section IV, the manufacturing and assembly errors, and even a slight variation in the operating conditions can lead to inconsistent performance of the proposed linear modulation. Since in large-scale applications, the consistency of valves are hardly guaranteed, and it is impossible to calibrate the characteristics of each valve manually. The unexpected inconsistency may impact the overall performance of the hydraulic control system. Thus, an additional controller guaranteeing actuators' consistency is required for robustness enhancement of the linear differential pressure modulation.

V. Control Precision Enhancement Through Load Pressure Feedback

In order to compensate for the performance inconsistency of the linear pressure drop control brought by manufacturing errors, varying conditions, and disturbances, a closed-loop feedback control for load pressure high-precision modulation is to be developed. Because of the ability to address hard

nonlinearity and the good robust performance with a fast response [29], a sliding mode control (SMC) scheme is adopted.

A. Sliding mode controller design

Based on the procedures introduced in [30], the SMC-based control law for the linear differential pressure modulation is developed as follows in detail.

The control objective of the system is to track the expected load pressure by the real wheel cylinder pressure. Thus, the error term is defined as:

$$e = p_w - p_{w,ref} \tag{23}$$

where, $p_{w,ref}$ is the desired load pressure in each wheel cylinder. p_w is the actual value of the wheel pressure.

The following sliding surface equation is chosen:

$$S = e + \lambda \int e dt \tag{24}$$

where, λ is a positive gain.

In order to guarantee that control law derives the system trajectories to the sliding surface, the Lyapunov direct method is used. The Lyapunov function is chosen as:

$$V = \frac{1}{2} SS \tag{25}$$

To ensure the stability of the system, the derivative of the Lyapunov function should satisfy the following condition:

$$\dot{V} = S\dot{S} \le 0 \tag{26}$$

Thus, when $\dot{S} = 0$, and based on equation (22)-(25), and the following control law can be obtained.

$$i_{ref,eq} = \frac{\pi R_v^2 (\cos\alpha)^2}{K_i} \left(\lambda^{-1} \dot{p}_{w,ref} - \lambda^{-1} \dot{p}_w + p_m - p_w + \frac{K_s (x_0 + x_m)}{\pi R_v^2 (\cos\alpha)^2} \right) \tag{27}$$

In order to satisfy the sliding condition, a discontinuous term sgn(S) is added to the above equation, and the SMC-based control law with linear pressure drop modulation for the inlet valve can be written as:

$$i_{ref} = \frac{\pi R_v^2 (\cos\alpha)^2}{K_i} \left(\lambda^{-1} \dot{p}_{w,ref} - \lambda^{-1} \dot{p}_w + p_m - p_w + \frac{K_s (x_0 + x_m)}{\pi R_v^2 (\cos\alpha)^2} \right) + k \,\mathrm{sgn}(S) \tag{28}$$

where, k>0 is a positive control gain. Sgn(S) is the sign function, and it equals to 1, 0, and -1, when the corresponding element of S is larger than 0, equals to 0, and is less than 0, respectively.

Remark 2: It is well known that in standard SMC, the discontinuous sign function, sgn(S), may cause chatter when the state trajectories are approaching the sliding surfaces [31], [32]. To avoid this phenomenon, the discontinuous term in equation (28) is replaced by the continuous function S, which removes the chatter from the control input [33], [34], as shown in equation (29).

$$i_{ref,eq} = \frac{\pi R_v^2 (\cos\alpha)^2}{K_i} \left(\lambda^{-1} \dot{p}_{w,ref} - \lambda^{-1} \dot{p}_w + p_m - p_w + \frac{K_s (x_0 + x_m)}{\pi R_v^2 (\cos\alpha)^2} \right) + kS \tag{29}$$

Thus, the developed sliding mode controller for feedback modulation of the load pressure is shown in Fig. 13. And the values of the tuning parameters are taken as λ=3 and k=0.1, respectively.

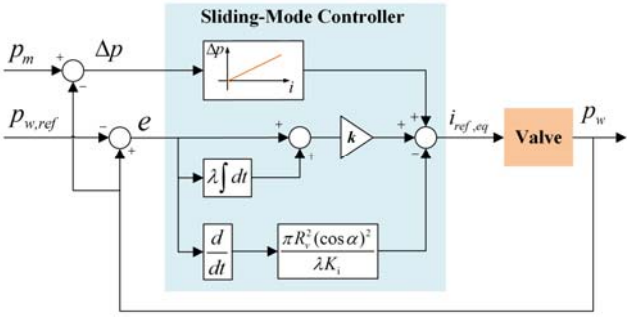

Fig. 13. Sliding mode control based load pressure feedback modulation.

B. SMC based closed-loop modulation verification and discussion

To test and verify the sliding mode controller based linear pressure drop modulation developed above, tests are carried out as follows.

Firstly, three valves with slightly different set-up in key parameters, indicating manufacturing and assembly errors or variation in working condition, are selected and used as the inlet valves in the tests, in order to represent inconsistent responses of the linear differential pressure modulation. Valve 1 is the one with original parameters showing in Table 1. Valve 2 is with the modified spool diameter of 1.688 mm, and valve 3 is with a modified current-force coefficient K_i of 4.8, which indicates a different coil turn number or a distinguished working temperature. The distinguished characteristics of the linear relationship between pressure-drop and coil current for the above three valves in their critical open equilibrium states are shown in Fig. 14.

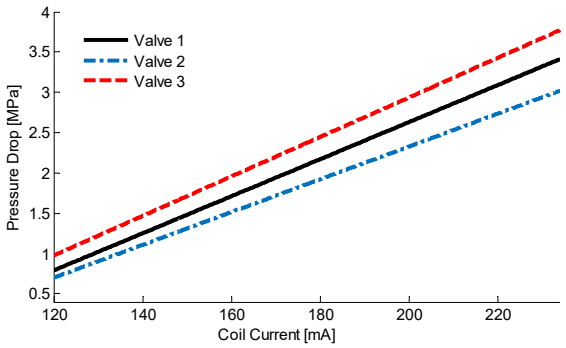

Fig. 14. Different characteristics of the linear relationship between pressure drop and coil current for the three selected valves.

1) Open-loop linear pressure drop control test

As a baseline, the open loop control solely relying on the linearity between coil current and the pressure drop is firstly tested. The control input is coil current, which is modulated according to the equation (21). A same pre-calibrated look-up table of the linear relation between coil current and the pressure drop, i.e. the one obtained by testing the reference valve 1, is applied in the three different channels. And a dynamical reference load pressure is required to be tracked. According to the open loop control test results illustrated in Fig. 15 (a), the load pressure responses of the three channels are far different in these three channels. The pressure in channel 2 is about 0.7 MPa higher than that in the channel 3. This is because of the

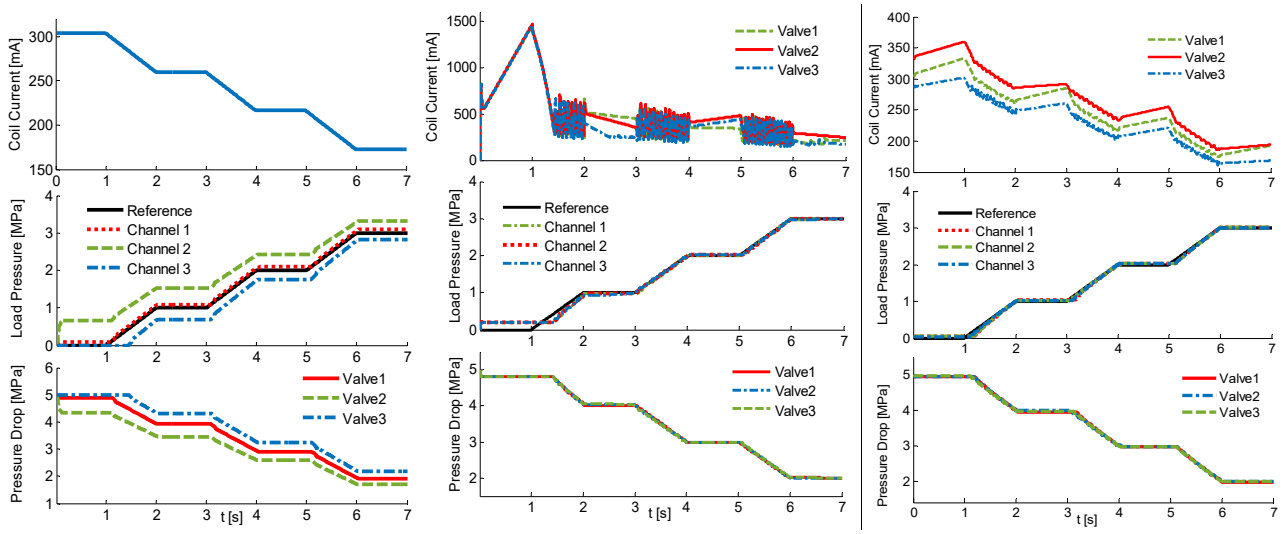

Fig. 15. Results of the dynamical load pressure tracking responses: (a) under open-loop linear pressure drop control; (b) under SMC without linear pressure drop modulation; (c) under the SMC-based closed loop linear pressure drop modulation.

distinctive pressure drop linearity caused by different parameters or environmental conditions. It also indicates that the open-loop control is not sufficient, and a feedback control of the load pressure is required for achieving a high-precision modulation.

2) SMC without linear pressure drop modulation

In order to evaluate the proposed modulation method, it is also necessary to compare the results of the proposed controller with a classic sliding mode controller without linear pressure drop modulation. Thus, a sliding mode controller which was also developed for hydraulic switching valve and presented in [17] is taken as another baseline and tested. For this controller, the control input is still coil current. According to the test results shown in Fig. 15 (b), without considering the proposed linear relationship between pressure drop and coil current, under the modulation of this sliding mode controller, the coil current is regulated dynamically for each valve. Although the load pressures in the three channels finally converge to the reference value, there are some gaps between the actual pressures and the expected one at initial phase, affecting the control performance. Besides, during pressure modulation, the coil currents are regulated frequently and the average values are relatively high, which are not desirable for the operation of automotive electronic components.

3) SMC-based linear pressure drop modulation test

Although the same look-up table for the open loop linear differential pressure control law is still in use, the sliding mode control scheme is added to compensate the valve's inconsistency and improve modulation accuracy. The control input is modulated according to equation (29). Based on the test results shown in Fig. 15 (c), under the SMC-based closed loop modulation, the coil current is regulated dynamically for each valve. Taking the 1st second as an example, the coil currents in channel 1-3 are in controlled increased, other than being held in the open-loop tests. Besides, the developed SMC algorithm regulates the input current based on the present load pressure in each channel independently. Thus, the coil current in channel 2 is 50 mA higher than that in the channel 3, which is different from the same regulation applied in the baseline tests. The distinguished pressure drop linearity is then adaptively compensated, and the load pressure is precisely modulated and converged to the same level in each channel, removing the unexpected valve inconsistency.

C.Performance comparison of the proposed modulation with conventional controls

The advances of the proposed SMC-based linear differential pressure modulation is evident from a comparison with PWM control, which is the most widely used modulation method for switching valves. In order to evaluate the pressure modulation accuracy, the root mean square error (RMSE) between the referenced and real pressures are adopted as evaluation parameter. The HiL test results of the RMSE values of the load pressure under different control methods are listed in Table 2.

In addition, the proposed SMC-based closed loop modulation enables a high-precision linear control of the hydraulic pressure utilizing the low-cost on/off valve, instead of the proportional valve, which requires a higher cost and larger space for its application in automotive braking system.

TABLE 2
COMPARISON OF DIFFERENT PRESSURE MODULATION METHODS

Modulation Method	RMSE [MPa]	Accuracy Improvement
PWM pressure control	5.292×10^{-2}	-
Open-loop linear pressure drop control	1.218×10^{-2}	76.98%
SMC without linear pressure drop modulation	1.526×10^{-2}	71.16%
SMC-based linear pressure drop control	5.866×10^{-3}	88.92%

D.Robustness analysis of the SMC-based modulation

Since the temperature affects the curve of the linear correspondence significantly, hence the robustness of the proposed controller under different temperature conditions is required to be investigated. The tracking performance of the developed SMC-based modulation is tested under +24℃, +13℃ and +3℃, respectively. Based on the test results presented in

Fig. 16, as the temperature rises, the controller increases the control effort, i.e. the coil current, accordingly. The control effects are remained the same with different temperatures, showing the good robustness of the proposed controller.

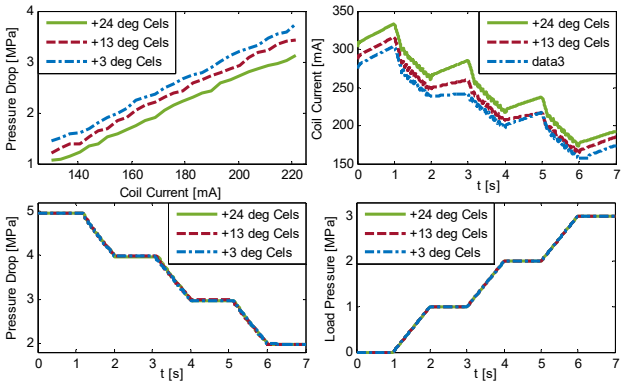

Fig. 16. Test results of the dynamical load pressure tracking responses under different temperature conditions.

VI. Conclusion

In this paper, a novel high-precision hydraulic pressure modulation method based on linear pressure drop control for switching valves was proposed. Based on the developed dynamical models of the hydraulic brake system with valve dynamics, the linear correlation between the differential pressure and the coil current in valve critical open equilibrium state was theoretically illustrated at first, and experimentally verified on the hardware-in-the-loop test rig as well. The control performance under different input pressures and varied coil currents were explored and analyzed. The sensitivity of the proposed modulation on key structure parameters and environmental temperatures were also studied. Furthermore, in order to achieve better robustness and precision for the linear pressure drop modulation, a sliding mode control based closed loop algorithm scheme was developed. Tests and comparisons with existing controls validated the effectiveness and superior performance of the proposed SMC-based method.

Further work will be carried out in the following areas: application of the linear pressure drop control in vehicle braking control, such as anti-lock brake control and brake blending control, and live tests of solenoid valves under the proposed novel modulation.

References

[1] S. A. Ali, A. Christen, S. Begg, and N. Langlois, "Continuous-Discrete Time-Observer Design for State and Disturbance Estimation of Electro-Hydraulic Actuator Systems," IEEE Transactions on Industrial Electronics, vol. 63, pp. 4314-4324, 2016.

[2] L. Wu, P. Shi, and X. Su. Sliding mode control of uncertain parameter-switching hybrid systems. John Wiley & Sons, 2014.

[3] Abdel-baqi, A. Nasiri, and P. Miller, "Dynamic Performance Improvement and Peak Power Limiting Using Ultracapacitor Storage System for Hydraulic Mining Shovels," IEEE Transactions on Industrial Electronics, vol. 62, pp. 3173-3181, 2015.

[4] Y. Lin, Y. Shi and R. Burton, "Modeling and robust discrete-time sliding mode control design for a fluid power electrohydraulic actuator (EHA) system," IEEE/ASME Trans. Mechatronics, vol. 18, 2013.

[5] F. Meng, H. Zhang, D. Cao, and H. Chen, "System Modeling, Coupling Analysis, and Experimental Validation of a Proportional Pressure Valve With Pulsewidth Modulation Control," IEEE/ASME Transactions on Mechatronics, vol. 21, pp. 1742-1753, 2016.

[6] C. Lv, J. Zhang, and Y. Li, "Extended-Kalman-filter-based regenerative and friction blended braking control for electric vehicle equipped with axle motor considering damping and elastic properties of electric powertrain," Vehicle System Dynamics, vol. 52, pp. 1372-1388, 2014.

[7] H. An, J. Liu, C. Wang, and L. Wu, "Disturbance Observer-Based Antiwindup Control for Air-Breathing Hypersonic Vehicles," IEEE Transactions on Industrial Electronics, vol. 63, pp. 3038-3049, 2016.

[8] J. J. Castillo, J. A. Cabrera, et al, "A novel electrohydraulic brake system with tire-road friction estimation and continuous brake pressure control," IEEE Transactions on Industrial Electronics, vol.63, pp.1863-1875, 2016.

[9] X. Liu, Y. Shi, and D. Constantinescu, "Robust Distributed Model Predictive Control of Constrained Continuous-Time Nonlinear Systems Using Two-Layer Invariant Sets," Journal of Dynamic Systems, Measurement, and Control, vol. 138, pp. 061004, 2016.

[10] J. Ko, S. Ko, H. Son, B. Yoo, J. Cheon, and H. Kim, "Development of Brake System and Regenerative Braking Cooperative Control Algorithm for Automatic-Transmission-Based Hybrid Electric Vehicles," IEEE Transactions on Vehicular Technology, vol. 64, pp. 431-440, 2015.

[11] X. Huang and J. Wang, "Model predictive regenerative braking control for lightweight electric vehicles with in-wheel motors," Proceedings of the Institution of Mechanical Engineers, Part D: Journal of Automobile Engineering, vol. 226, pp. 1220-1232, 2012.

[12] J. N. Bae, Y. E. Kim, Y. W. Son, H. S. Moon, C. H. Yoo, and J. Lee, "Self-Excited Induction Generator as an Auxiliary Brake for Heavy Vehicles and Its Analog Controller," IEEE Transactions on Industrial Electronics, vol. 62, pp. 3091-3100, 2015.

[13] B. K. Sarkar, J. Das, R. Saha, S. Mookherjee, and D. Sanyal, "Approaching Servoclass Tracking Performance by a Proportional Valve-Controlled System," IEEE/ASME Transactions on Mechatronics, vol. 18, pp. 1425-1430, 2013.

[14] E. Prasetiawan, Z. Rong, and A. Alleyne, "Fundamental performance limitations for a class of electronic two-stage proportional flow valves," in American Control Conference, vol.5, pp. 3955-3960, 2001.

[15] T. Radpukdee and P. Jirawattana, "Uncertainty learning and compensation: An application to pressure tracking of an electro-hydraulic proportional relief valve," Control Engineering Practice, vol. 17, pp. 291-301, 2009.

[16] P. Mercorelli, "A Motion Sensorless Control for Intake Valves in Combustion Engines," IEEE Transactions on Industrial Electronics, 2016, in press.

[17] X. Zhao, L. Li, J. Song, C. Li, and X. Gao, "Linear Control of Switching Valve in Vehicle Hydraulic Control Unit Based on Sensorless Solenoid Position Estimation," IEEE Transactions on Industrial Electronics, vol. 63, pp. 4073-4085, 2016.

[18] C. Lv, J. Zhang, Y. Li, D. Sun, and Y. Yuan, "Hardware-in-the-loop simulation of pressure-difference-limiting modulation of the hydraulic brake for regenerative braking control of electric vehicles," Proceedings of the Institution of Mechanical Engineers, Part D: Journal of Automobile Engineering, vol. 228, pp. 649-662, 2014.

[19] K. Ahn and S. Yokota, "Intelligent switching control of pneumatic actuator using on/off solenoid valves," Mechatronics, vol. 15, pp. 683-702, 2005.

[20] E. Lisowski and G. Filo, "Automated heavy load lifting and moving system using pneumatic cushions," Automation in Construction, vol. 50, pp. 91-101, 2015.

[21] L. Lu and B. Yao, "Energy-Saving Adaptive Robust Control of a Hydraulic Manipulator Using Five Cartridge Valves With an Accumulator," IEEE Transactions on Industrial Electronics, vol. 61, pp. 7046-7054, 2014.

[22] P. Eyabi and G. Washington, "Modeling and sensorless control of an electromagnetic valve actuator," Mechatronics, vol. 16, pp. 159-175, 2006.

[23] F. Meng, P. Shi, H. R. Karimi, and H. Zhang, "Optimal design of an electro-hydraulic valve for heavy-duty vehicle clutch actuator with certain constraints," Mechanical Systems and Signal Processing, vol. 68–69, pp. 491-503, 2016.

[24] J. Zhang, C. Lv, X. Yue, et al, "Study on a linear relationship between limited pressure difference and coil current of on/off valve and its influential factors," ISA Transactions, vol. 53, pp. 150-161, 2014.

[25] G. S. Lee, H. J. Sung, H. C. Kim, and H. W. Lee, "Flow Force Analysis of a Variable Force Solenoid Valve for Automatic Transmissions," Journal of Fluids Engineering, vol. 132, pp. 031103, 2010.

[26] N. D. Manring and S. Zhang, "Pressure Transient Flow Forces for Hydraulic Spool Valves," Journal of Dynamic Systems, Measurement, and Control, vol. 134, pp. 034501, 2012.

[27] R. Rajamani, “Vehicle dynamics and control”, Springer, 2011.
[28] W.H. Hayt, and B.A. John, “Engineering electromagnetics”, vol. 7, New York: McGraw-Hill, 2001.
[29] D. Swaroop, J. K. Hedrick, P. P. Yip, and J. C. Gerdes, "Dynamic surface control for a class of nonlinear systems," IEEE Transactions on Automatic Control, vol. 45, pp. 1893-1899, 2000.
[30] B., Song, J.K. Hedrick, Dynamic surface control of uncertain nonlinear systems: An LMI Approach, Springer, 2011.
[31] H. Imine, A. Benallegue, T. Madani, and S. Srairi, "Rollover Risk Prediction of Heavy Vehicle Using High-Order Sliding mode Observer: Experimental Results," IEEE Transactions on Vehicular Technology, vol. 63, pp. 2533-2543, 2014.
[32] C. Lv, J. Zhang, Y. Li, and Y. Yuan, "Mode-switching-based active control of a powertrain system with non-linear backlash and flexibility for an electric vehicle during regenerative deceleration," Proceedings of the Institution of Mechanical Engineers, Part D: Journal of Automobile Engineering, vol. 229, pp. 1429-1442, 2015.
[33] A. Fazeli, M. Zeinali, and A. Khajepour, "Application of Adaptive Sliding Mode Control for Regenerative Braking Torque Control," IEEE/ASME Transactions on Mechatronics, vol. 17, pp. 745-755, 2012.
[34] C. Lv, J. Zhang, Y. Li, and Y. Yuan, "Directional-stability-aware brake blending control synthesis for over-actuated electric vehicles during straight-line deceleration," Mechatronics, vol. 38, pp. 121-131, 2016.

Chen Lv is currently a research fellow at Advanced Vehicle Engineering Center, Cranfield University, UK. He received the Ph.D. degree from Tsinghua University, China, in 2016. From 2014 to 2015, he was a joint PhD researcher at EECS Dept., University of California, Berkeley. His research focuses on vehicle control and intelligence, where he has contributed over 40 papers and 11 China patents. Dr. Lv serves as a Guest Editor for Int. J. of Powertrains, and an Associate Editor for Int. J. of Electric and Hybrid Vehicles, Int. J. of Vehicle Systems Modelling and Testing, and Int. J. of Science and Engineering for Smart Vehicles. He received the Highly Commended Paper Award of IMechE UK in 2012, the NSK Outstanding Mechanical Engineering Paper Award in 2014, the China SAE Outstanding Paper Award in 2015, the 1st Class Award of China Automotive Industry Scientific and Technological Invention in 2015, and the Tsinghua University Outstanding Doctoral Thesis Award in 2016.

Hong Wang is currently a Postdoc Fellow of Mechanical and Mechatronics Engineering with the University of Waterloo. She received his Ph.D. degree in Beijing Institute of Technology in China in 2015. Her research focuses on the component sizing, modeling of hybrid powertrains and power management control strategies design for Hybrid electric vehicles; intelligent control theory and application; autonomous vehicles.

Dongpu Cao received the Ph.D. degree from Concordia University, Canada, in 2008. He is currently a Senior Lecturer at Advanced Vehicle Engineering Center, Cranfield University, UK. His research focuses on vehicle dynamics, control and intelligence, where he has contributed more than 90 publications and 1 US patent. He received the ASME AVTT’2010 Best Paper Award and 2012 SAE Arch T. Colwell Merit Award. Dr. Cao serves as an Associate Editor for IEEE TRANSACTIONS ON INTELLIGENT TRANSPORTATION SYSTEMS, IEEE TRANSACTIONS ON VEHICULAR TECHNOLOGY, IEEE TRANSACTIONS ON INDUSTRIAL ELECTRONICS and ASME JOURNAL OF DYNAMIC SYSTEMS, MEASUREMENT, AND CONTROL. He has been a Guest Editor for IEEE/ASME TRANSACTIONS ON MECHATRONICS, VEHICLE SYSTEM DYNAMICS, and IEEE TRANSACTIONS ON HUMAN-MACHINE SYSTEMS. He serves on the SAE International Vehicle Dynamics Standards Committee and a few ASME, SAE, IEEE technical committees.

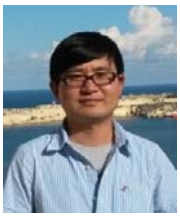

High-precision hydraulic pressure control based on linear pressure-drop modulation in valve critical equilibrium state

Lv, Chen

2017-09-11

Lv C, Wang H, Cao DP. (2017) High-precision hydraulic pressure control based on linear pressure-drop modulation in valve critical equilibrium state, IEEE Transactions on Industrial Electronics, Volume 64, Issue 10, October 2017, pp. 7984-7993

http://dx.doi.org/10.1109/TIE.2017.2694414